MONITORING PLASMA OVER-ETCHING OF WAFER-BONDED MICROSTRUCTURES

Raj K. Gupta, Charles H. Hsu, M. A. Schmidt, and S. D. Senturia

Microsystems Technology Laboratories
Department of Electrical Engineering and Computer Science
Massachusetts Institute of Technology, Cambridge, MA 02139 USA

JUNE 1996

© 1995 Foundation for Sensor and Actuator Technology. Personal use of this material is permitted. However, permission to reprint/republish this material for advertising or promotional purposes or for creating new collective works for resale or redistribution to servers or lists, or to reuse any copyrighted component of this work must be obtained from the Foundation for Sensor and Actuator Technology, Stockholm, Sweden.

MONITORING PLASMA OVER-ETCHING OF WAFER-BONDED MICROSTRUCTURES

Raj K. Gupta, Charles H. Hsu, M. A. Schmidt, and S. D. Senturia

Microsystems Technology Laboratories, Department of Electrical Engineering and Computer Science
Massachusetts Institute of Technology, Cambridge, MA 02139 USA

SUMMARY

We have demonstrated that wafer-level probing of electrostatic pull-in test structures provides a means to monitor MEMS process uniformity and integrity. Test structures, which have proved to be useful in determining MEMS material properties, are used here to identify and quantify a non-uniform plasma over-etch used in the final release of silicon wafer-bonded microstructures. MEMCAD simulations confirm that the changes in test structure geometry do indeed account for the behavior seen experimentally.

INTRODUCTION

Measurement of electrostatic pull-in voltage has been proposed as a method for material property measurement and process monitoring [1,2]. In our group's previous work [3,4], we presented numerical and analytical models for the electrostatic pull-in of cantilevers, fixed-fixed beams, and circular diaphragms, and demonstrated the use of some of these structures for monitoring process uniformity and for extraction of material properties. The approach used an analytical expression which relates the pull-in voltage to structural dimensions and material properties through two intermediate parameters, the stress parameter S_n and bending parameter B_n, where n indexes the structure type. These quantities are found by non-linear least-squares fitting of pull-in voltage as a function of structure length or radius. They depend linearly on residual stress (for S_n) or Young's Modulus (for B_n), and on powers of critical dimensions varying with a given test structure. In this paper, we show how pull-in measurements on fixed-fixed beams of two different widths signaled a fabrication problem during the plasma-etch release step.

EXPERIMENTAL RESULTS

We studied fixed-fixed beam test structures designed for a nominal thickness of 14.5μm and a gap of 1.0μm using MIT's sealed-cavity wafer-bonded technology [5]. Because these wafer-bonded structures have relatively low residual stress [5], the stress parameter S_2 is small and will not contribute to mechanical stiffness. In this limit, a bending-dominated analytic form [4] was found for the pull-in voltage V_{PI} as shown in equation (1):

$$V_{PI} = \sqrt{\frac{11.16\,B_2}{0.97^2\,\varepsilon_o\,L^4\left(1+0.42\,g/w\right)}} \quad (1)$$

The bending-parameter B_2 is defined as Et^3g^3. The Young's Modulus E, the beam thickness t, and the gap g, are assumed to be uniform for a given beam. And finally, L is the length, and ε_o is the permittivity. Implicit in this estimate is a uniform width w, across a beam cross-section.

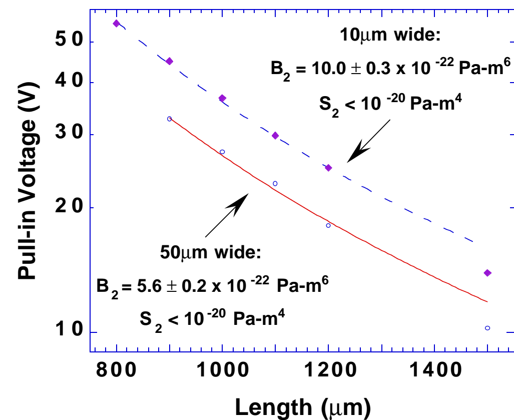

Figure 1: Experimental pull-in voltages (points) vs. fixed-fixed beam length. Fitted lines are obtained by the closed-form expressions for pull-in [4]. Nominal B_2 value is 6.3×10^{-22} Pa-m^6.

Figure 1 shows the pull-in versus length for two sets of parallel and adjacent fixed-fixed beams with nominal widths of 10μm and 50μm. When the experimental data are fit to equation (1), the bending parameters can be determined to better than 10%. For the 50μm-wide beams, B_2 is close to the expected nominal value based on an E of 169GPa in the [110] direction of a <100> plane of single crystal silicon [6]. B_2 for the 10μm-wide beams is twice as large. This discrepancy suggests a problem with the sample geometry.

One possible explanation is an over-etch resulting from a prolonged anisotropic CCl_4/SF_6 plasma-etch release of the microstructures. This concept is illustrated in Figure 2, where etched dimensions are magnified for clarity. The over-etch is expected to have a limited encroachment under the beam. Therefore, one might expect gaps under narrow

beams to be more affected than wide beams. SEM cross-sections of a 10µm- and 50µm-wide cantilever are shown in Figure 3. They are both positioned above substrate landing pads. Although there was an observable over-etch of the p-substrate pads, the n-silicon beam undersides remained unaffected and stayed relatively flat.

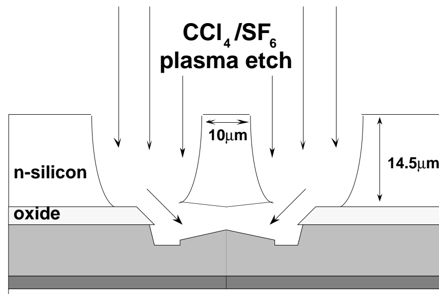

Figure 2: Illustration of plasma attacking the underside of a wafer-bonded beam in cross-section. Etch profiles and dimensions are exaggerated.

Figure 4 shows Dektak™ surface profile measurements using a 12.5µm diamond radius tip across a 10µm- and a 50µm-wide beam substrate pad and trench regions. The dotted lines align differences in height between the top of the oxide and the center of the substrate pads, to a vertical resolution of 10Å. This distance is effectively the gap between the bottom of the beam and center of the pad. Gaps resulting from this are 1.08µm for the 50µm-wide beam and 1.22µm for the 10µm-wide beam. They show only a 50Å variation along the beam length. Dektak measurements also indicate a uniform thickness of 14.37µm of the mechanical layer across the wafer.

SEM photos are used to obtain an effective radius of curvature R of the pad regions along the beam width. R is 60µm (±5%) for the 10µm-wide beam. There is significantly less curvature on the wider beam. Thus, we will assume that the wide beams have the nominal geometry, and examine only the narrow beams in detail.

ANALYSIS

Because the electrostatic force is proportional to the inverse of the gap squared, we can calculate an effective uniform gap g_{eff} for any pull-in geometry, as follows:

$$g_{eff} = \left[\frac{1}{A} \int_A \frac{dxdy}{g(x,y)^2} \right]^{-1/2} \quad (2)$$

From equation (2), we find that the narrow beams have a $g_{eff} \approx 1.39$µm. This effective gap can inserted into the B_2 parameter to test whether it accounts for the observed experimental behavior. However, it is also necessary to correct for the trapezoidal beam cross-section, and this procedure is discussed below.

As a test case, consider a beam 1000µm long and 14.37µm thick, and assume a trapezoidal beam cross-section which is 10µm on top (w_t), and 17µm on bottom (w_b). To compute B_2, we must take into account the compliance of the non-uniform cross-sectional width of the beam, and note that the electrostatic force resides mainly on

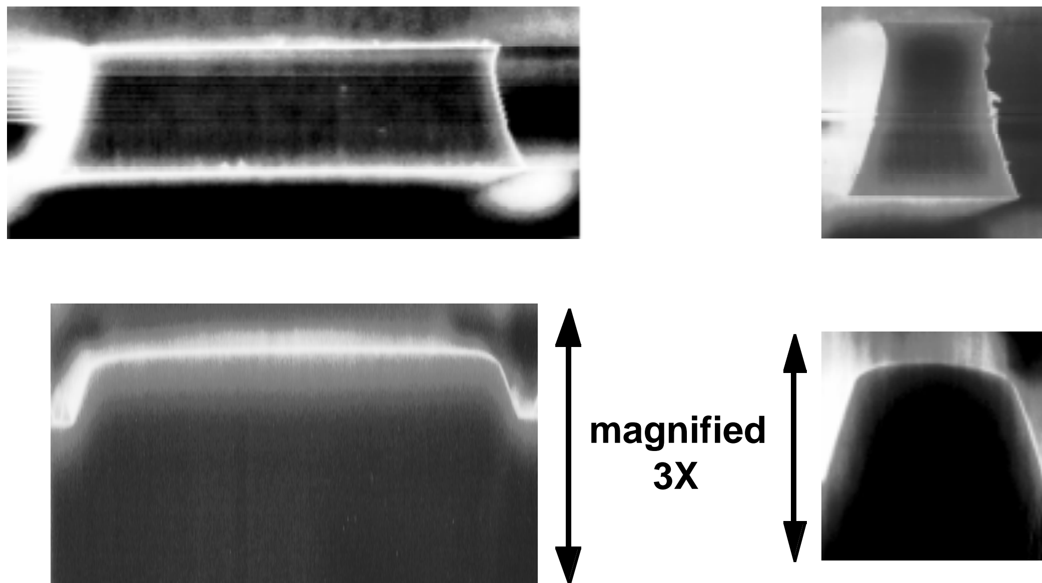

Figure 3: SEM cross-sections of 50µm-(left) and 10µm-wide(right) cantilevers over a corresponding substrate landing pad. The width of 10µm-wide beam underside is 17µm and that of its substrate landing pad is approximately 15µm. We approximate the rounding of the 15µm-wide pad to have a radius of curvature of 60µm. Note also the relative flatness of the beam undersides.

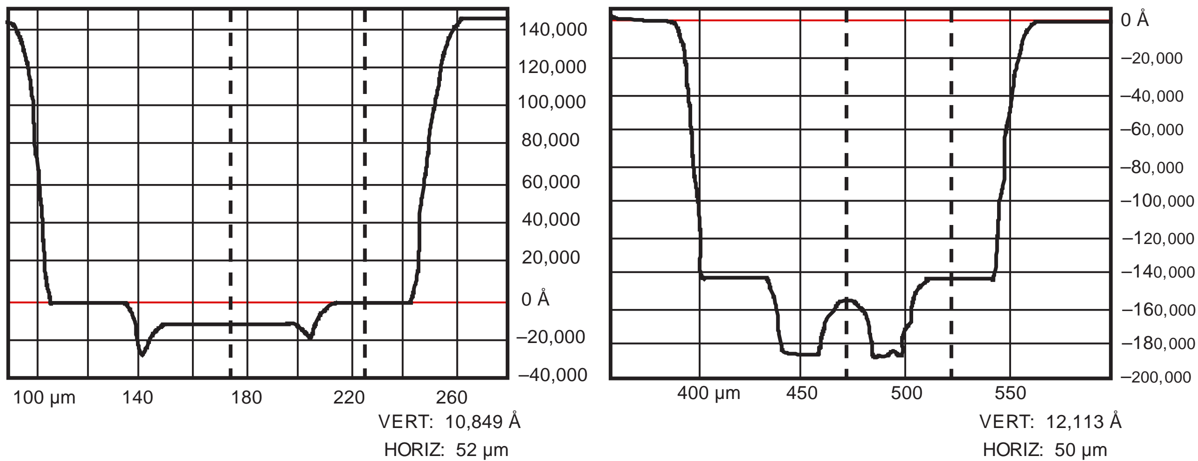

Figure 4: Dektak™ surface profile measurements of p-substrate contacts of a 50µm-(left) and a 10µm-wide(right) fixed-fixed beam. The dotted lines align difference in vertical height of the center of the pads to the top of the exposed oxide. This difference, the gap, is 1.08µm on the left and 1.21µm on the right. (Vertical scale is in Å, and horizontal in µm. Vertical resolution is 10Å.)

the 17µm-wide face of the bottom of the beam. To do this, we factor in the ratio of the moment of areas of the trapezoidal cross-section to an equivalent rectangular beam whose width is given by w_b. The equation for B_2 is updated, as follows:

$$B_2 = Et^3 g_{eff}{}^3 \left(\frac{w_t{}^2 + 4w_t w_b + w_b{}^2}{3w_b(w_t + w_b)} \right) \quad (3)$$

When g_{eff} = 1.39µm is substituted into equation (3), we obtain a B_2 equal to 10.5 x 10^{-22} Pa-m^6. This is very close to experimentally determined value of 10.0 x 10^{-22} Pa-m^6 in Figure 1. And equation (1) can now be used with the new B_2 to show that the calculated pull-in voltage of 36.6 is in excellent agreement with the experimentally determined pull-in voltage of 35.9 volts.

Pull-in results were also analyzed using a 2-D MATLAB™ numerical finite-difference model with fringing-field correction, similar to those in [4] and [8]. In this case, the value of g_{eff} was used for the gap at zero voltage. Full 3-D simulations were also performed using CoSolve-EM [7] within the MIT MEMCAD system. In the 3-D simulation, the rounded substrate pad can be explicitly represented. A minimum gap of 1.22µm together with a radius of curvature of 60µm were used for the landing-pad geometry, as shown in Figure 5.

The calculated pull-in voltages are 36.5 volts and 36.3 volts for the 2-D and 3-D models, respectively, which agree closely with each other, and with the experimental value of 35.9 volts. In the case of the 3-D MEMCAD simulation, a mesh-convergence study showed that the mechanical stiffness of the meshed beam and the electrostatic forces were calculated within about 5% error, and since the pull-in voltage goes approximately as the square root of the stiffness [4], pull-in errors resulting from the mesh are of order 2.5%. A similar analysis showed that the 2-D MATLAB meshed errors were less than 1%. Figure 6 shows the deflection at the beam center as a function of voltage.

The small remaining discrepancy between simulation and experiment may result from the assumed trapezoidal cross-section, which should be slightly stiffer than the actual cross-section seen in the SEM’s of Figure 3. Nevertheless, we observe that when the geometry is reasonably approximated, the theory works well.

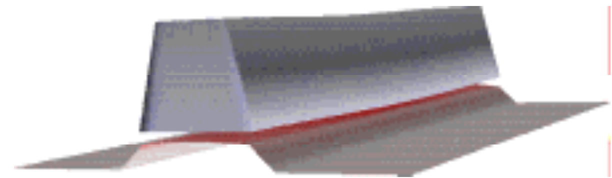

Figure 5: A deformed geometry of a narrow fixed-fixed beam under electrostatic loading using MEMCAD. Beam thickness is 14.37µm, and it is 10µm wide on the top, and 17µm wide at the bottom. The radius of curvature of the rounded ground plane is 60µm. The axis along the 1000µm beam length is scaled 1/10 to allow for better viewing.

CONCLUSIONS

The ability to monitor relatively small differences in geometry by using non-destructive, wafer-level probing of test structures has proven very useful. By observing a change in the effective gap, it is possible to be quantitative about the degree of the plasma over-etch found in silicon wafer-bonded micromachined processes. Furthermore, once good geometry information is obtained, successful and accurate modelling by various techniques is possible.

The results of this work have also helped to focus effort on a process redesign which involves leaving a masking layer (SiO_2) in the sealed cavity to eliminate the over-etch problem.

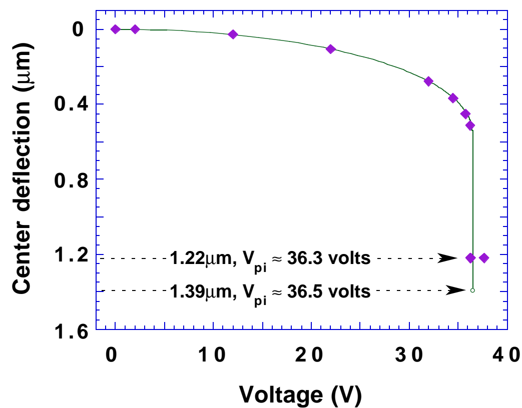

Figure 6. Comparison of 2-D (solid line) and 3-D (points) simulations for a narrow beam with trapezoidal cross-section. The 2-D simulation used g_{eff} = *1.39µm, while the 3-D simulation used the geometry of Figure 5 with a minimum gap at the center of the landing pad of 1.22µm.*

ACKNOWLEDGMENTS

This work was sponsored in part by the Semiconductor Research Corporation (Contract 94-SC-309) and by ARPA (Contract J-FBI-92-196). The authors are indebted to Peter Osterberg and Dr. John Gilbert for assistance with the simulation methods.

REFERENCES

[1] K. E. Petersen, "Dynamic Micromechanics on Silicon: Techniques and Devices," *IEEE Trans. on Electron Devices*, **ED-25** (1978) pp. 1241-1250.

[2] K. Najafi and K. Suzuki, "A Novel Technique and Structure for the Measurement of Intrinsic Stress and Young's Modulus of Thin Films," *Proc. MEMS 1989* (Salt Lake City, Feb. 1989) pp. 96-97.

[3] P. M. Osterberg, H. Yie, X. Cai, J. White and S. D. Senturia, "Self-Consistent Simulation and Modeling of Electrostatically Deformed Diaphragms," *Proc. MEMS 1994* (Oiso, JAPAN, January 1994) pp. 28-32.

[4] P. M. Osterberg, R. Gupta, J. R. Gilbert and S. D. Senturia, "Quantitative Models for the Measurement of Residual Stress, Poisson's Ratio and Young's Modulus Using Electrostatic Pull-in of Beams and Diaphragms," *Proc. 1994 Solid-State Sensor and Actuator Workshop* (Hilton Head, SC, June 1994) pp. 184-188.

[5] C. H. Hsu and M. A. Schmidt, "Micromachined Structures Fabricated Using Wafer-Bonded Sealed Cavity Process," *Proc. 1994 Solid-State Sensor and Actuator Workshop* (Hilton Head, SC, June 1994) pp. 151-155.

[6] W. A. Brantley, "Calculated elastic constants for stress problems associated with semiconductor devices," *J. Appl. Phys.*, **44** (1973) pp. 534-535.

[7] J. R. Gilbert, R. Legtenberg and S. D. Senturia, "3D Coupled Electro-mechanics for MEMS: Applications of CoSolve-EM," *Proc. MEMS 1995* (Amsterdam, the Netherlands, February 1995) pp. 122-127.

[8] B. E. Artz and L. W. Cathey, "A Finite Element Method for Determining Structural Displacements Resulting from Electrostatic Forces," *IEEE Solid-State Sensor and Actuator Workshop* (Hilton Head, SC, June 1992) pp. 190-193.